EUROPEAN ORGANIZATION FOR NUCLEAR RESEARCH (CERN)

Measurement of the ratio of branching fractions of the decays $\Lambda_b^0 \to \psi(2S)\Lambda$ and $\Lambda_b^0 \to J/\psi\,\Lambda$

LHCb collaboration[†]

Abstract

Using pp collisions corresponding to $3\,\text{fb}^{-1}$ integrated luminosity, recorded by the LHCb experiment at centre-of-mass energies of 7 and 8 TeV, the ratio of branching fractions

$$\mathcal{B}(\Lambda_b^0 \to \psi(2S)\Lambda)/\mathcal{B}(\Lambda_b^0 \to J/\psi\,\Lambda) = 0.513 \pm 0.023\,(\text{stat}) \pm 0.016\,(\text{syst}) \pm 0.011\,(\mathcal{B})$$

is determined. The first uncertainty is statistical, the second is systematic and the third is due to the external branching fractions used.

Submitted to JHEP

[†]Authors are listed at the end of this paper.

1 Introduction

The LHCb collaboration has observed many $\Lambda_b^0 \to J/\psi\, X$ [1–7] and $\Lambda_b^0 \to \psi(2S)X$ decays [5, 8], where X indicates a final-state particle system. Ratios of branching fractions of b-hadron decays into $\psi(2S)X$ and $J/\psi\, X$ provide useful information on the production of charmonia in b-hadron decays. These ratios can be used to test factorisation of amplitudes. The ATLAS collaboration has previously measured the ratio of the branching fractions to be $\mathcal{B}(\Lambda_b^0 \to \psi(2S)\Lambda)/\mathcal{B}(\Lambda_b^0 \to J/\psi\, \Lambda) = 0.501 \pm 0.033\,(\text{stat}) \pm 0.019\,(\text{syst})$ [9]. This result differs by $2.8\,\sigma$ from a theoretical prediction in the framework of the covariant quark model, $\mathcal{B}(\Lambda_b^0 \to \psi(2S)\Lambda)/\mathcal{B}(\Lambda_b^0 \to J/\psi\, \Lambda) = 0.8 \pm 0.1$ [10, 11], and with similar measurements in the B^0 system, $\mathcal{B}(B^0 \to \psi(2S)K_s^0)/\mathcal{B}(B^0 \to J/\psi\, K_s^0) = 0.71 \pm 0.06$ [12]. In this paper the measurement of the branching fraction of the decay $\Lambda_b^0 \to \psi(2S)\Lambda$ by LHCb is presented. Throughout this paper, the notation of a decay always implies the inclusion of the charge-conjugate process. Determining the branching fraction of $\Lambda_b^0 \to \psi(2S)\Lambda$ decays relative to the branching fraction of $\Lambda_b^0 \to J/\psi\, \Lambda$ cancels most experimental uncertainties. A measurement with improved precision helps to better understand this possible discrepancy and sets new constraints on the available form-factor models [11].

2 LHCb detector

The LHCb detector [13, 14] is a single-arm forward spectrometer covering the pseudorapidity range $2 < \eta < 5$, designed for the study of particles containing b or c quarks. The detector includes a high-precision tracking system consisting of a silicon-strip vertex detector (VELO) surrounding the pp interaction region [15], a large-area silicon-strip detector located upstream of a dipole magnet with a bending power of about $4\,\text{Tm}$, and three stations of silicon-strip detectors and straw drift tubes [16] placed downstream of the magnet. The tracking system provides a measurement of the momentum, p, of charged particles with a relative uncertainty that varies from 0.5% at low momentum to 1.0% at $200\,\text{GeV}/c$. The minimum distance of a track to a primary vertex (PV), the impact parameter (IP), is measured with a resolution of $(15 + 29/p_\text{T})\,\mu\text{m}$, where p_T is the component of the momentum transverse to the beam, in GeV/c. Different types of charged hadrons are distinguished using information from two ring-imaging Cherenkov detectors [17]. Photons, electrons and hadrons are identified by a calorimeter system consisting of scintillating-pad and preshower detectors, an electromagnetic calorimeter and a hadronic calorimeter. Muons are identified by a system composed of alternating layers of iron and multiwire proportional chambers [18]. The online event selection is performed by a trigger [19], which consists of a hardware stage, based on information from the muon system, followed by a software stage, which applies a full event reconstruction. In the simulation, pp collisions are generated using PYTHIA [20] with a specific LHCb configuration [21]. Decays of hadronic particles are described by EVTGEN [22]. The interaction of the generated particles with the detector, and its response, are implemented using the GEANT4 toolkit [23] as described in Ref. [24].

3 Event selection and selection efficiencies

The J/ψ and $\psi(2S)$ charmonium states, collectively called ψ, are reconstructed through their decay into two muons. Two tracks not originating from any PV, that are identified as oppositely charged muons, are required to form a good vertex. These muons have to fulfil various trigger requirements. At the hardware stage an event is required to contain a muon with high p_{T} or two muons with a large product of their respective p_{T} values. At the software stage further requirements are placed on the p_{T}, momenta and IP of the muons. The reconstructed ψ masses must be within $\pm 100\,\mathrm{MeV}/c^2$ of their known masses [12].

The Λ candidates are reconstructed by combining a pion and a proton candidate. Due to its long lifetime, the Λ baryon can decay either inside or outside the VELO. The pion and proton can be reconstructed including hits from the VELO (long track) or without (downstream track). Combinations where the track types of pion and proton differ are not considered. Due to different momentum resolutions of these track types, some selection requirements differ between the two samples. The pion and proton candidates are required to have high momentum ($> 2\,\mathrm{GeV}/c$) and high p_{T} and the tracks must be displaced from any PV. In addition, long-track proton candidates must be consistent with the proton hypothesis. The invariant mass of the pion and proton combination has to be compatible with the known Λ mass [12] and both tracks must come from a common vertex. Furthermore, the Λ candidate is required to have a decay time longer than 2 ps.

The Λ_b^0 candidate is reconstructed by combining the ψ and the Λ candidates and requiring that they form a common vertex. The PV that fits best to the Λ_b^0 flight direction is assigned as associated PV. It is required that the Λ_b^0 momentum points back to this PV and its decay vertex is significantly displaced from this PV. Additional requirements are imposed using a kinematic fit with constrained ψ and Λ masses. For downstream-track candidates the reconstructed Λ decay time using this fit must be longer than 9 ps. The χ^2/ndf of this kinematic fit is required to be smaller than $36/6$ for long-track candidates and smaller than $26/6$ for downstream-track candidates.

After the selection, about 1% of all events contain multiple candidates. Among these multiple candidates a single candidate is retained using a random but reproducible procedure. To ensure a precise efficiency determination, fiducial cuts on the Λ_b^0 baryon, $p_{\mathrm{T}}(\Lambda_b^0) < 20\,\mathrm{GeV}/c$ and $2 < \eta(\Lambda_b^0) < 4.5$ are applied.

The signal efficiency is evaluated separately for each channel and track type, using simulations and crosschecked with data. The simulation assumes unpolarised decays but is corrected using theory predictions [10] for both decay channels. Sources of inefficiencies are the geometrical acceptance of the detector, the trigger, the track reconstruction, and the candidate selection. The last three efficiencies depend on the kinematics of the Λ_b^0 baryon, which is not perfectly simulated. To account for the mismodelling, these efficiencies are determined in bins of $p_{\mathrm{T}}(\Lambda_b^0)$ and $\eta(\Lambda_b^0)$. The same binning scheme, consisting of seven bins for each of the two variables, is used for both decay channels. The binning scheme is designed such that all bins are uniformly populated, with at least 100 entries in each bin. The resulting efficiency for a given candidate is determined by linear interpolation of the binned efficiency model to reduce effects arising from the choice of the binning scheme. For the interpolation, the mean value in each bin is used and additional bins are added to ensure interpolation at the boundaries. The resulting efficiency functions together with the distribution of the corresponding signal candidates are shown in Fig. 1.
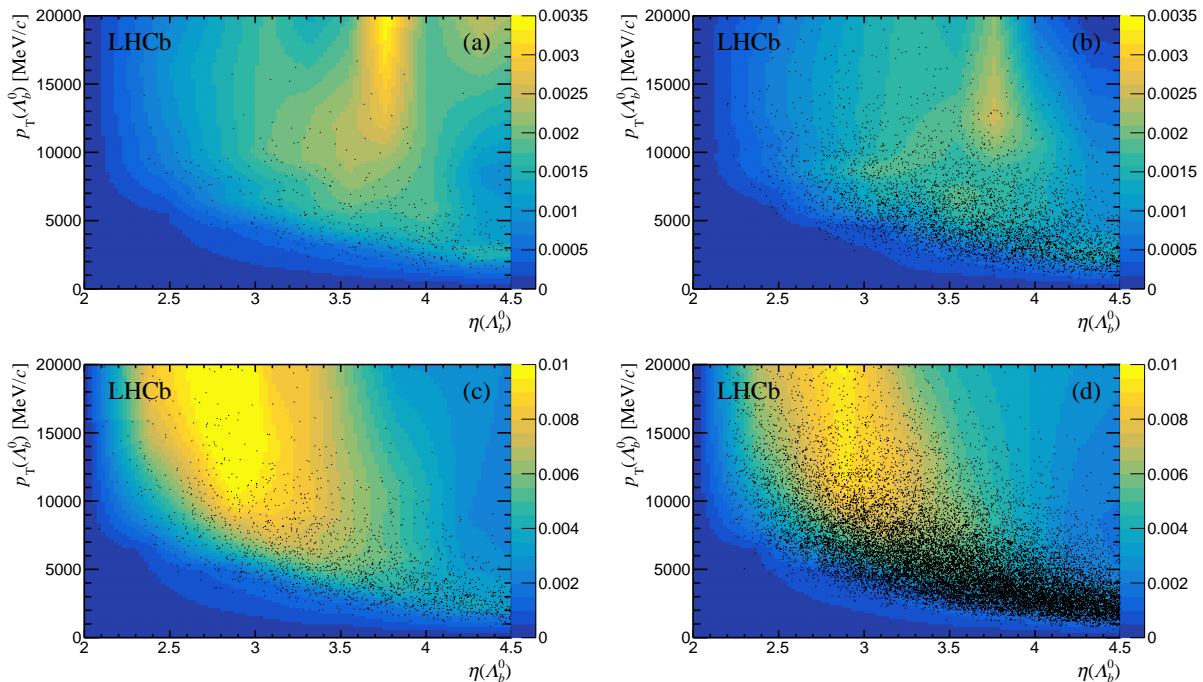
Figure 1: Interpolated efficiency function for long-track candidates for (a) $\Lambda_b^0 \to \psi(2S)\Lambda$ and (b) $\Lambda_b^0 \to J/\psi\Lambda$ and for downstream-track candidates for (c) $\Lambda_b^0 \to \psi(2S)\Lambda$ and (d) $\Lambda_b^0 \to J/\psi\Lambda$ candidates. The distribution of the candidates on data is shown with black dots (each dot refers to one candidate).

4 Signal yield determination

The signal yield is determined using an extended unbinned maximum likelihood fit to the reconstructed Λ_b^0 mass in the range 5350 to 5750 MeV/c^2 separately for both decay channels and track types. The fit model for the reconstructed Λ_b^0 mass consists of several components. The signal is modelled with a double-sided Hypatia function [25], where the tail parameters are fixed to values obtained from fits to the simulation. The combinatorial background is modelled with an exponential function. A background due to $B^0 \to \psi K_S^0$ decays, where the K_S^0 meson decays to two pions and one of the pions is misidentified as a proton, is vetoed in the long-track sample by applying additional particle identification requirements. In the downstream-track sample this component is modelled with a kernel-density estimation using a Gaussian kernel [26] obtained from simulated $B^0 \to \psi K_S^0$ decays. Another source of background is $\Xi_b^- \to \psi\Xi^-$ decays, where the Ξ^- baryon decays to $\Lambda\pi^-$ and the pion is not reconstructed. Contributions from this background source are negligible in the long-track sample due to the sum of the large lifetimes of the Ξ and the Λ baryons. Thus, the $\Lambda \to p\pi^-$ decay only happens in less than 2% of the $\Xi_b^- \to \psi\Xi^-$ decays inside the VELO. In the downstream-track sample this background is modelled with a kernel-density estimation using a Gaussian kernel obtained from simulated $\Xi_b^- \to \psi\Xi^-$ decays. The number of observed signal events is determined from a fit to unweighted invariant-mass distributions. The resulting fit is shown in Fig. 2, separately for long and downstream tracks, and the resulting yields for each data sample are shown in Table 1. In a second fit, the efficiency-corrected yields are obtained assigning to each candidate a weight given by the inverse of the efficiency. This fit to the two weighted invariant-mass
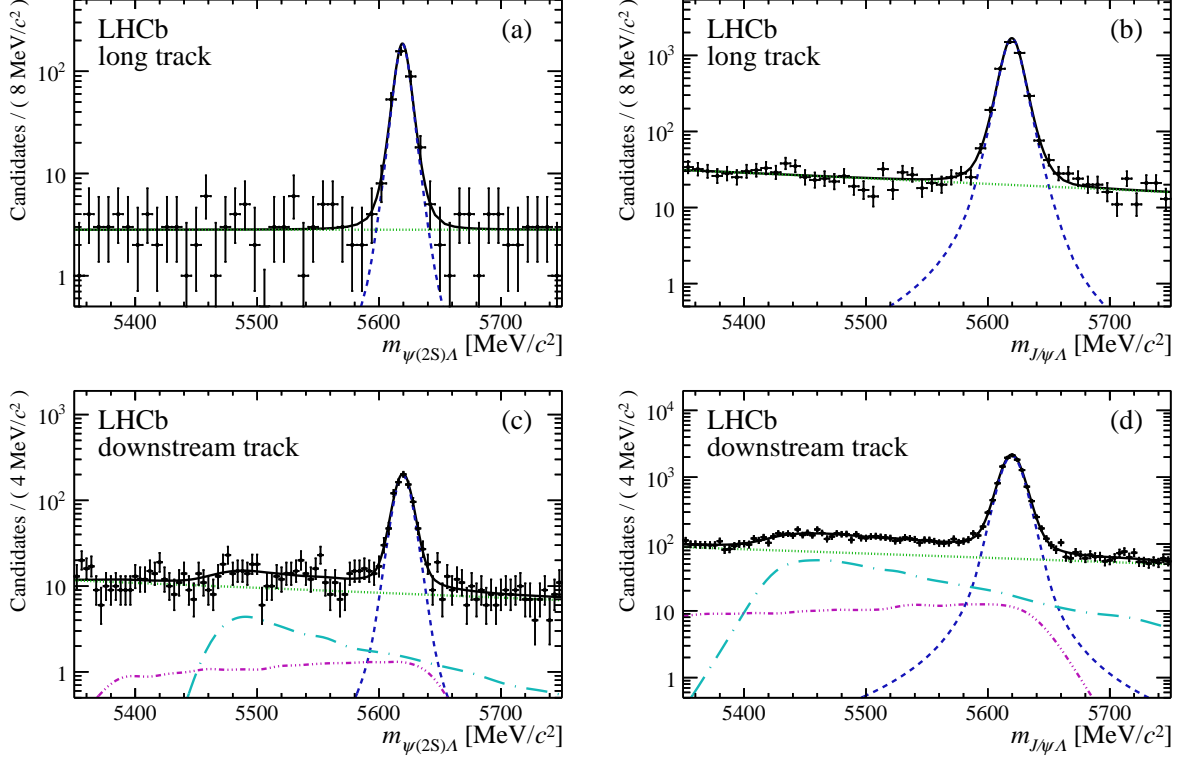
3

Figure 2: Fits to the (unweighted) invariant-mass distributions of long-track candidates for (a) $\Lambda_b^0 \to \psi(2S)\Lambda$ and (b) $\Lambda_b^0 \to J/\psi\Lambda$ and for downstream-track candidates for (c) $\Lambda_b^0 \to \psi(2S)\Lambda$ and (d) $\Lambda_b^0 \to J/\psi\Lambda$ candidates. The signal (blue, dashed), the combinatorial background (green, dotted), the $B^0 \to \psi K_S^0$ background (cyan, long-dash-dotted) and the $\Xi_b^- \to \psi\Xi^-$ background (violet, dash-triple-dotted) are indicated.

Table 1: Yields from the invariant-mass fits in the range 5350 to 5750 MeV/c^2 of (top) $\Lambda_b^0 \to J/\psi\Lambda$ decays and (bottom) $\Lambda_b^0 \to \psi(2S)\Lambda$ decays for each component.

track type	$\Lambda_b^0 \to J/\psi\Lambda$	$B^0 \to J/\psi K_S^0$	$\Xi_b^- \to J/\psi\Xi^-$	combinatorial
downstream	$11\,090 \pm 120$	$2\,330 \pm 210$	800 ± 400	$6\,790 \pm 240$
long	$3\,800 \pm 60$	–	–	$1\,130 \pm 40$
	$\Lambda_b^0 \to \psi(2S)\Lambda$	$B^0 \to \psi(2S)K_S^0$	$\Xi_b^- \to \psi(2S)\Xi^-$	combinatorial
downstream	819 ± 33	160 ± 60	60 ± 90	920 ± 60
long	317 ± 19	–	–	140 ± 13

distributions is shown in Fig. 3 for each data sample and the resulting efficiency-corrected signal yields for each data sample are reported in Table 2.
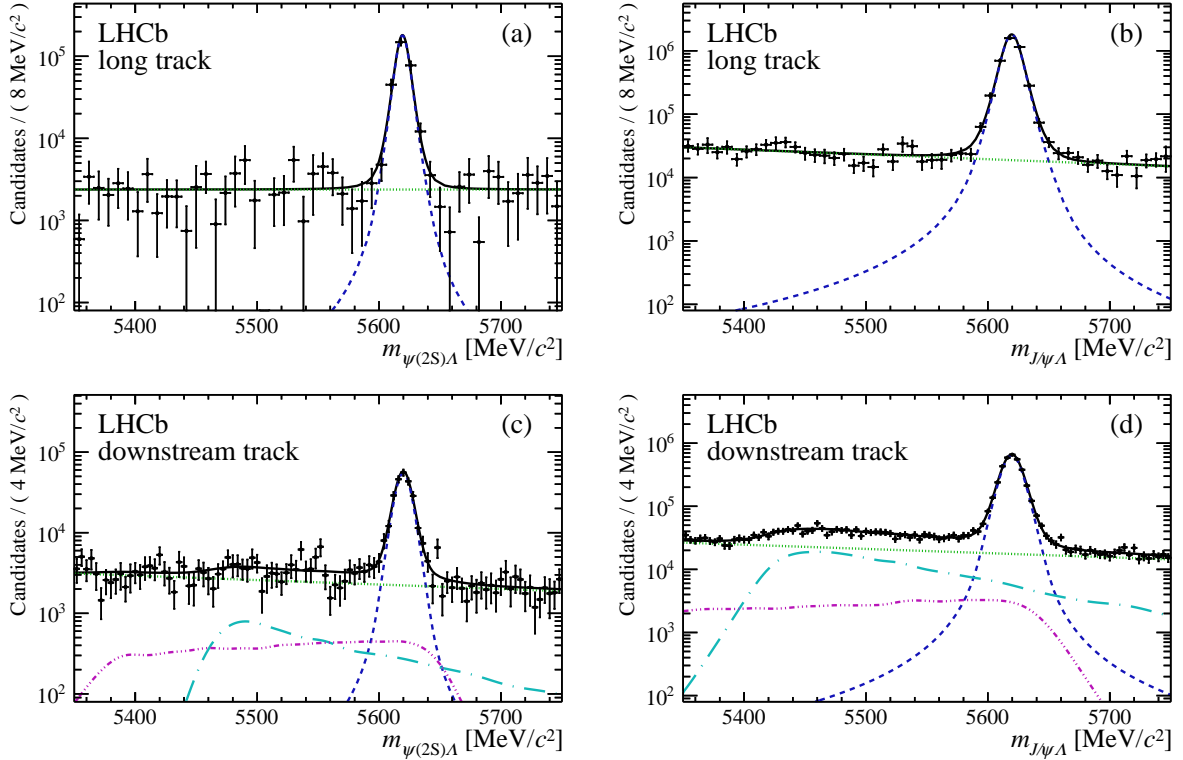
4

Figure 3: Fits to the weighted invariant-mass distributions of long-track candidates for (a) $\Lambda_b^0 \to \psi(2S)\Lambda$ and (b) $\Lambda_b^0 \to J/\psi\,\Lambda$ and for downstream-track candidates for (c) $\Lambda_b^0 \to \psi(2S)\Lambda$ and (d) $\Lambda_b^0 \to J/\psi\,\Lambda$ candidates. The signal (blue, dashed), the combinatorial background (green, dotted), the $B^0 \to \psi K_S^0$ background (cyan, long-dash-dotted) and the $\Xi_b^- \to \psi \Xi^-$ background (violet, dash-triple-dotted) are indicated.

Table 2: Efficiency-corrected yields of $\Lambda_b^0 \to \psi(2S)\Lambda$ and $\Lambda_b^0 \to J/\psi\,\Lambda$ signal decays from the fit to the weighted invariant mass for both track types.

track type	$N_{\Lambda_b^0 \to \psi(2S)\Lambda}$	$N_{\Lambda_b^0 \to J/\psi\,\Lambda}$
downstream	$223\,000 \pm 13\,000$	$3\,320\,000 \pm 50\,000$
long	$280\,000 \pm 18\,000$	$3\,980\,000 \pm 80\,000$

5 Result

The ratio of branching fractions of $\Lambda_b^0 \to \psi(2S)\Lambda$ and $\Lambda_b^0 \to J/\psi\,\Lambda$ decays is determined separately for long- and downstream-track candidates using

$$\frac{\mathcal{B}(\Lambda_b^0 \to \psi(2S)\Lambda)}{\mathcal{B}(\Lambda_b^0 \to J/\psi\,\Lambda)} = \frac{N_{\Lambda_b^0 \to \psi(2S)\Lambda}}{N_{\Lambda_b^0 \to J/\psi\,\Lambda}} \cdot \frac{\mathcal{B}(J/\psi \to \mu^+\mu^-)}{\mathcal{B}(\psi(2S) \to \mu^+\mu^-)}, \tag{1}$$

where N is the number of efficiency-corrected signal candidates, and $\mathcal{B}(J/\psi \to \mu^+\mu^-)$ and $\mathcal{B}(\psi(2S) \to \mu^+\mu^-)$ are the known branching fractions of the ψ mesons to two muons [12]. Assuming lepton universality, the value for the branching fraction of $\psi(2S)$ into two electrons, $\mathcal{B}(\psi(2S) \to e^+e^-) = (0.793 \pm 0.017)\%$ [12], is used in the calculation due to its lower uncertainty compared to the muon decay. Using the value for the branching fraction

Table 3: Relative systematic uncertainties on the ratio of branching fractions.

	value
Simulated dataset size	1.1 %
Binning choice	1.6 %
Trigger efficiency	1.2 %
Fit model	1.6 %
Simulation correction	1.3 %
$\mathcal{B}(c\bar{c} \to \ell\ell)$	2.2 %
total	3.8 %
total without $\mathcal{B}(c\bar{c} \to \ell\ell)$	3.1 %

of J/ψ into two muons, $\mathcal{B}(J/\psi \to \mu^+\mu^-) = (5.961 \pm 0.033)\%$ [12] and the efficiency-corrected signal yields, given in Table 2, the ratios of branching fractions for both track types are calculated to be

$$\left[\frac{\mathcal{B}(\Lambda_b^0 \to \psi(2S)\Lambda)}{\mathcal{B}(\Lambda_b^0 \to J/\psi\,\Lambda)}\right]_{\text{long track}} = 0.528 \pm 0.036,$$

$$\left[\frac{\mathcal{B}(\Lambda_b^0 \to \psi(2S)\Lambda)}{\mathcal{B}(\Lambda_b^0 \to J/\psi\,\Lambda)}\right]_{\text{downstream track}} = 0.504 \pm 0.029,$$

where the statistical uncertainty only includes the uncertainty on the measured signal yields. The results for the two classes of tracks are in good agreement and are combined using a weighted average into

$$\frac{\mathcal{B}(\Lambda_b^0 \to \psi(2S)\Lambda)}{\mathcal{B}(\Lambda_b^0 \to J/\psi\,\Lambda)} = 0.513 \pm 0.023.$$

6 Systematic uncertainties

The sources of systematic uncertainty are summarised in Table 3. The effect of each of these sources on the measured ratio is evaluated independently and is quoted as a relative uncertainty on the measured ratio of branching fractions. These relative uncertainties are summed in quadrature to obtain the total systematic uncertainty.

All efficiencies are evaluated from simulated data, therefore the precision is limited by the size of the simulated dataset. This effect is determined by varying the binned efficiencies within binomial uncertainties and re-evaluating the efficiency-weighted signal yield. The result varies by 1.1 %, which is assigned as the systematic uncertainty. The effect of the chosen number of bins in both dimensions for the efficiency determination is determined by varying the numbers of bins between five and ten in each dimension independently. The largest difference compared to the the baseline result is a change of 1.6% in the ratio of yields, which is assigned as systematic uncertainty. To estimate a systematic uncertainty for the trigger efficiency, kinematically similar channels with higher rates, $B^+ \to J/\psi\,K^+$ and $B^+ \to \psi(2S)K^+$, are used [27]. The resulting trigger efficiency on data is compatible with that obtained on simulation, but the systematic uncertainty due to the size of the sample used for this method is 1.2 %. The effect of using alternative

fit models that describe the mass distributions are evaluated using pseudoexperiments. Candidates are generated using an alternative model and then fitted with the default model. The 1.6% relative difference between the fitted and generated yield is assigned as systematic uncertainty. The used correction on the helicity angles in simulation is taken from theory predictions [10]. An alternative approach is to use the measured distributions from data and this leads to a difference of 1.3% to the baseline result, which is assigned as systematic uncertainty. The effect of neglecting peaking backgrounds for long-track candidates is evaluated by including the $\Xi_b^- \to \psi \Xi^-$ and $B^0 \to \psi K_S^0$ components in the long-track sample fits and letting their yields vary freely. The resulting yields for these components are compatible with zero and the variation of the signal yield is negligible. Summing these uncertainties in quadrature leads to a systematic uncertainty of 3.1%. Another uncertainty arises from the external values for the branching fractions of the charmonium to two muon decays, which is 2.2% [12].

The consistency of the results has been checked by repeating the analysis separately with datasets with different magnet polarities and years of data taking. In another crosscheck, the $B^0 \to \psi K_S^0$ background is vetoed instead of being included in the fit. None of these checks shows a significant deviation from the baseline result.

7 Conclusion

In summary the ratio of branching fractions is determined to be

$$\frac{\mathcal{B}(\Lambda_b^0 \to \psi(2S)\Lambda)}{\mathcal{B}(\Lambda_b^0 \to J/\psi \Lambda)} = 0.513 \pm 0.023 \,(\text{stat}) \pm 0.016 \,(\text{syst}) \pm 0.011 \,(\mathcal{B}),$$

where the first uncertainty is statistical, the second is systematic and the third is due to the uncertainty of the used ψ meson branching fractions to two leptons [12]. This measurement is compatible within one standard deviation with the measurement from the ATLAS collaboration [9] and has a better precision. It confirms the discrepancy with the covariant quark model theory predictions [10, 11] and sets additional constraints on available models.

Acknowledgements

References

[1] LHCb collaboration, R. Aaij *et al.*, *Measurements of the $\Lambda_b^0 \to J/\psi \Lambda$ decay amplitudes and the Λ_b^0 polarisation in pp collisions at $\sqrt{s} = 7~TeV$*, Phys. Lett. **B724** (2013) 27, arXiv:1302.5578.

[2] LHCb collaboration, R. Aaij *et al.*, *Observation of the $\Lambda_b^0 \to J/\psi p\pi^-$ decay*, JHEP **07** (2014) 103, arXiv:1406.0755.

[3] LHCb collaboration, R. Aaij *et al.*, *Observation of $J/\psi p$ resonances consistent with pentaquark states in $\Lambda_b^0 \to J/\psi pK^-$ decays*, Phys. Rev. Lett. **115** (2015) 072001, arXiv:1507.03414.

[4] LHCb collaboration, R. Aaij *et al.*, *Study of the productions of Λ_b^0 and $\overline{B}^0$ hadrons in pp collisions and first measurement of the $\Lambda_b^0 \to J/\psi pK^-$ branching fraction*, Chin. Phys. **C40** (2016) 011001, arXiv:1509.00292.

[5] LHCb collaboration, R. Aaij *et al.*, *Observation of $\Lambda_b^0 \to \psi(2S)pK^-$ and $\Lambda_b^0 \to J/\psi \pi^+\pi^- pK^-$ decays and a measurement of the Λ_b^0 baryon mass*, JHEP **05** (2016) 132, arXiv:1603.06961.

[6] LHCb collaboration, R. Aaij *et al.*, *Model-independent evidence for $J/\psi p$ contributions to $\Lambda_b^0 \to J/\psi pK^-$ decays*, Phys. Rev. Lett. **117** (2016) 082002, arXiv:1604.05708.

[7] LHCb collaboration, R. Aaij *et al.*, *Evidence for exotic hadron contributions to $\Lambda_b^0 \to J/\psi p\pi^-$ decays*, Phys. Rev. Lett. **117** (2016) 082003, arXiv:1606.06999.

[8] LHCb collaboration, R. Aaij *et al.*, *Observation of the decay $\Lambda_b^0 \to \psi(2S)p\pi^-$*, JHEP **08** (2018) 131, arXiv:1806.08084.

[9] ATLAS collaboration, G. Aad *et al.*, *Measurement of the branching ratio $\Gamma(\Lambda_b^0 \to \psi(2S)\Lambda)/\Gamma(\Lambda_b^0 \to J/\psi \Lambda)$ with the ATLAS detector*, Phys. Lett. **B751** (2015) 63, arXiv:1507.08202.

[10] T. Gutsche *et al.*, *Polarization effects in the cascade decay $\Lambda_b^0 \to \Lambda(\to p\pi^-) + J/\psi(\to \ell^+\ell^-)$ in the covariant confined quark model*, Phys. Rev. **D88** (2013) 114018, arXiv:1309.7879.

[11] T. Gutsche *et al.*, *Towards an assessment of the ATLAS data on the branching ratio $\Gamma(\Lambda_b^0 \to \psi(2S)\Lambda)/\Gamma(\Lambda_b^0 \to J/\psi \Lambda)$*, Phys. Rev. **D92** (2015) 114008, arXiv:1510.02266.

[12] Particle Data Group, M. Tanabashi *et al.*, *Review of particle physics*, Phys. Rev. **D98** (2018) 030001.

[13] LHCb collaboration, A. A. Alves Jr. *et al.*, *The LHCb detector at the LHC*, JINST **3** (2008) S08005.

[14] LHCb collaboration, R. Aaij *et al.*, *LHCb detector performance*, Int. J. Mod. Phys. **A30** (2015) 1530022, `arXiv:1412.6352`.

[15] R. Aaij *et al.*, *Performance of the LHCb Vertex Locator*, JINST **9** (2014) P09007, `arXiv:1405.7808`.

[16] R. Arink *et al.*, *Performance of the LHCb Outer Tracker*, JINST **9** (2014) P01002, `arXiv:1311.3893`.

[17] M. Adinolfi *et al.*, *Performance of the LHCb RICH detector at the LHC*, Eur. Phys. J. **C73** (2013) 2431, `arXiv:1211.6759`.

[18] A. A. Alves Jr. *et al.*, *Performance of the LHCb muon system*, JINST **8** (2013) P02022, `arXiv:1211.1346`.

[19] R. Aaij *et al.*, *The LHCb trigger and its performance in 2011*, JINST **8** (2013) P04022, `arXiv:1211.3055`.

[20] T. Sjöstrand, S. Mrenna, and P. Skands, *A brief introduction to PYTHIA 8.1*, Comput. Phys. Commun. **178** (2008) 852, `arXiv:0710.3820`; T. Sjöstrand, S. Mrenna, and P. Skands, *PYTHIA 6.4 physics and manual*, JHEP **05** (2006) 026, `arXiv:hep-ph/0603175`.

[21] I. Belyaev *et al.*, *Handling of the generation of primary events in Gauss, the LHCb simulation framework*, J. Phys. Conf. Ser. **331** (2011) 032047.

[22] D. J. Lange, *The EvtGen particle decay simulation package*, Nucl. Instrum. Meth. **A462** (2001) 152.

[23] Geant4 collaboration, J. Allison *et al.*, *Geant4 developments and applications*, IEEE Trans. Nucl. Sci. **53** (2006) 270; Geant4 collaboration, S. Agostinelli *et al.*, *Geant4: A simulation toolkit*, Nucl. Instrum. Meth. **A506** (2003) 250.

[24] M. Clemencic *et al.*, *The LHCb simulation application, Gauss: Design, evolution and experience*, J. Phys. Conf. Ser. **331** (2011) 032023.

[25] D. Martínez Santos and F. Dupertuis, *Mass distributions marginalized over per-event errors*, Nucl. Instrum. Meth. **A764** (2014) 150, `arXiv:1312.5000`.

[26] K. S. Cranmer, *Kernel estimation in high-energy physics*, Comput. Phys. Commun. **136** (2001) 198, `arXiv:hep-ex/0011057`.

[27] S. Tolk, J. Albrecht, F. Dettori, and A. Pellegrino, *Data driven trigger efficiency determination at LHCb*, CERN-LHCb-PUB-2014-039.

LHCb Collaboration

R. Aaij[42], B. Adeva[41], M. Adinolfi[48], Z. Ajaltouni[5], S. Akar[59], J. Albrecht[10], F. Alessio[42],
M. Alexander[53], A. Alfonso Albero[40], S. Ali[27], G. Alkhazov[33], P. Alvarez Cartelle[55],
A.A. Alves Jr[59], S. Amato[2], S. Amerio[23], Y. Amhis[7], L. An[3], L. Anderlini[17], G. Andreassi[43],
M. Andreotti[16,g], J.E. Andrews[60], R.B. Appleby[56], F. Archilli[27], J. Arnau Romeu[6],
A. Artamonov[39], M. Artuso[61], E. Aslanides[6], M. Atzeni[44], G. Auriemma[26], M. Baalouch[5],
I. Babuschkin[56], S. Bachmann[12], J.J. Back[50], A. Badalov[40,m], C. Baesso[62], S. Baker[55],
V. Balagura[7,b], W. Baldini[16], A. Baranov[37], R.J. Barlow[56], C. Barschel[42], S. Barsuk[7],
W. Barter[56], F. Baryshnikov[70], V. Batozskaya[31], V. Battista[43], A. Bay[43], L. Beaucourt[4],
J. Beddow[53], F. Bedeschi[24], I. Bediaga[1], A. Beiter[61], L.J. Bel[27], N. Beliy[63], V. Bellee[43],
N. Belloli[20,i], K. Belous[39], I. Belyaev[34,42], G. Bencivenni[18], E. Ben-Haim[8], S. Benson[27],
S. Beranek[9], A. Berezhnoy[35], R. Bernet[44], D. Berninghoff[12], E. Bertholet[8], A. Bertolin[23],
C. Betancourt[44], F. Betti[15], M.O. Bettler[42], Ia. Bezshyiko[44], S. Bifani[47], P. Billoir[8],
A. Birnkraut[10], A. Bizzeti[17,u], M. Bjørn[57], T. Blake[50], F. Blanc[43], S. Blusk[61], V. Bocci[26],
T. Boettcher[58], A. Bondar[38,w], N. Bondar[33], I. Bordyuzhin[34], S. Borghi[56,42], M. Borisyak[37],
M. Borsato[41], F. Bossu[7], M. Boubdir[9], T.J.V. Bowcock[54], E. Bowen[44], C. Bozzi[16,42], S. Braun[12],
J. Brodzicka[29], D. Brundu[22], E. Buchanan[48], C. Burr[56], A. Bursche[22,f], J. Buytaert[42],
W. Byczynski[42], S. Cadeddu[22], H. Cai[64], R. Calabrese[16,g], R. Calladine[47], M. Calvi[20,i],
M. Calvo Gomez[40,m], A. Camboni[40,m], P. Campana[18], D.H. Campora Perez[42], L. Capriotti[56],
A. Carbone[15,e], G. Carboni[25,j], R. Cardinale[19,h], A. Cardini[22], P. Carniti[20,i], L. Carson[52],
K. Carvalho Akiba[2], G. Casse[54], L. Cassina[20], M. Cattaneo[42], G. Cavallero[19,42,h], R. Cenci[24,t],
D. Chamont[7], M.G. Chapman[48], M. Charles[8], Ph. Charpentier[42], G. Chatzikonstantinidis[47],
M. Chefdeville[4], S. Chen[22], S.F. Cheung[57], S.-G. Chitic[42], V. Chobanova[41], M. Chrzaszcz[42],
A. Chubykin[33], P. Ciambrone[18], X. Cid Vidal[41], G. Ciezarek[42], F. Cindolo[15], P.E.L. Clarke[52],
M. Clemencic[42], H.V. Cliff[49], J. Closier[42], V. Coco[42], J. Cogan[6], E. Cogneras[5], V. Cogoni[22,f],
L. Cojocariu[32], P. Collins[42], T. Colombo[42], A. Comerma-Montells[12], A. Contu[22], G. Coombs[42],
S. Coquereau[40], G. Corti[42], M. Corvo[16,g], C.M. Costa Sobral[50], B. Couturier[42], G.A. Cowan[52],
D.C. Craik[58], A. Crocombe[50], M. Cruz Torres[1], R. Currie[52], F. Da Cunha Marinho[2],
C.L. Da Silva[73], E. Dall'Occo[27], J. Dalseno[48], C. D'Ambrosio[42], P. d'Argent[12], A. Davis[3],
O. De Aguiar Francisco[42], K. De Bruyn[42], S. De Capua[56], M. De Cian[12], J.M. De Miranda[1],
L. De Paula[2], M. De Serio[14,d], P. De Simone[18], J.A. de Vries[27], C.T. Dean[53], D. Decamp[4],
L. Del Buono[8], H.-P. Dembinski[11], M. Demmer[10], A. Dendek[30], D. Derkach[37], O. Deschamps[5],
F. Dettori[54], B. Dey[65], A. Di Canto[42], P. Di Nezza[18], H. Dijkstra[42], F. Dordei[42], M. Dorigo[42],
A.C. dos Reis[1], A. Dosil Suárez[41], L. Douglas[53], A. Dovbnya[45], K. Dreimanis[54], L. Dufour[27],
G. Dujany[8], P. Durante[42], J.M. Durham[73], D. Dutta[56], R. Dzhelyadin[39], M. Dziewiecki[12],
A. Dziurda[42], A. Dzyuba[33], S. Easo[51], M. Ebert[52], U. Egede[55], V. Egorychev[34],
S. Eidelman[38,w], S. Eisenhardt[52], U. Eitschberger[10], R. Ekelhof[10], L. Eklund[53], S. Ely[61],
S. Esen[27], H.M. Evans[49], T. Evans[57], A. Falabella[15], C. Färber[42], N. Farley[47], S. Farry[54],
D. Fazzini[20,i], L. Federici[25], M. Féo[27], D. Ferguson[52], G. Fernandez[40], P. Fernandez Declara[42],
A. Fernandez Prieto[41], F. Ferrari[15], L. Ferreira Lopes[43], F. Ferreira Rodrigues[2],
M. Ferro-Luzzi[42], S. Filippov[36], R.A. Fini[14], M. Fiorini[16,g], M. Firlej[30], C. Fitzpatrick[43],
T. Fiutowski[30], F. Fleuret[7,b], M. Fontana[22,42], F. Fontanelli[19,h], R. Forty[42], V. Franco Lima[54],
M. Frank[42], C. Frei[42], J. Fu[21,q], W. Funk[42], E. Furfaro[25,j], E. Gabriel[52], A. Gallas Torreira[41],
D. Galli[15,e], S. Gallorini[23], S. Gambetta[52], M. Gandelman[2], P. Gandini[21], Y. Gao[3],
L.M. Garcia Martin[72], J. García Pardiñas[41], J. Garra Tico[49], L. Garrido[40], P.J. Garsed[49],
D. Gascon[40], C. Gaspar[42], L. Gavardi[10], G. Gazzoni[5], D. Gerick[12], E. Gersabeck[56],
M. Gersabeck[56], T. Gershon[50], Ph. Ghez[4], S. Gianì[43], V. Gibson[49], O.G. Girard[43],
L. Giubega[32], K. Gizdov[52], V.V. Gligorov[8], C. Göbel[62], D. Golubkov[34], A. Golutvin[55,70],
A. Gomes[1,a], I.V. Gorelov[35], C. Gotti[20,i], E. Govorkova[27], J.P. Grabowski[12], R. Graciani Diaz[40],

L.A. Granado Cardoso[42], E. Graugés[40], E. Graverini[44], G. Graziani[17], A. Grecu[32], R. Greim[9], P. Griffith[22], L. Grillo[56], L. Gruber[42], B.R. Gruberg Cazon[57], O. Grünberg[67], E. Gushchin[36], Yu. Guz[39], T. Gys[42], T. Hadavizadeh[57], C. Hadjivasiliou[5], G. Haefeli[43], C. Haen[42], S.C. Haines[49], B. Hamilton[60], X. Han[12], T.H. Hancock[57], S. Hansmann-Menzemer[12], N. Harnew[57], S.T. Harnew[48], C. Hasse[42], M. Hatch[42], J. He[63], M. Hecker[55], K. Heinicke[10], A. Heister[9], K. Hennessy[54], P. Henrard[5], L. Henry[72], M. Heß[67], A. Hicheur[2], D. Hill[57], P.H. Hopchev[43], W. Hu[65], W. Huang[63], Z.C. Huard[59], W. Hulsbergen[27], T. Humair[55], M. Hushchyn[37], D. Hutchcroft[54], P. Ibis[10], M. Idzik[30], P. Ilten[47], A. Inyakin[39], R. Jacobsson[42], J. Jalocha[57], E. Jans[27], A. Jawahery[60], F. Jiang[3], M. John[57], D. Johnson[42], C.R. Jones[49], C. Joram[42], B. Jost[42], N. Jurik[57], S. Kandybei[45], M. Karacson[42], J.M. Kariuki[48], S. Karodia[53], N. Kazeev[37], M. Kecke[12], F. Keizer[49], M. Kelsey[61], M. Kenzie[49], T. Ketel[28], E. Khairullin[37], B. Khanji[12], C. Khurewathanakul[43], T. Kirn[9], S. Klaver[18], K. Klimaszewski[31], T. Klimkovich[11], S. Koliiev[46], M. Kolpin[12], R. Kopecna[12], P. Koppenburg[27], A. Kosmyntseva[34], S. Kotriakhova[33], M. Kozeiha[5], L. Kravchuk[36], M. Kreps[50], F. Kress[55], P. Krokovny[38,w], W. Krzemien[31], W. Kucewicz[29,l], M. Kucharczyk[29], V. Kudryavtsev[38,w], A.K. Kuonen[43], T. Kvaratskheliya[34,42], D. Lacarrere[42], G. Lafferty[56], A. Lai[22], A. Lanfranchi[18], C. Langenbruch[9], T. Latham[50], C. Lazzeroni[47], R. Le Gac[6], R. Lefèvre[5], A. Leflat[35,42], J. Lefrançois[7], F. Lemaitre[42], O. Leroy[6], T. Lesiak[29], B. Leverington[12], P.-R. Li[63,z], T. Li[3], Y. Li[7], Z. Li[61], X. Liang[61], T. Likhomanenko[69], R. Lindner[42], F. Lionetto[44], V. Lisovskyi[7], X. Liu[3], D. Loh[50], A. Loi[22], I. Longstaff[53], J.H. Lopes[2], D. Lucchesi[23,o], M. Lucio Martinez[41], H. Luo[52], A. Lupato[23], E. Luppi[16,g], O. Lupton[42], A. Lusiani[24], X. Lyu[63], F. Machefert[7], F. Maciuc[32], V. Macko[43], P. Mackowiak[10], S. Maddrell-Mander[48], O. Maev[33,42], K. Maguire[56], D. Maisuzenko[33], M.W. Majewski[30], S. Malde[57], B. Malecki[29], A. Malinin[69], T. Maltsev[38,w], G. Manca[22,f], G. Mancinelli[6], D. Marangotto[21,q], J. Maratas[5,v], J.F. Marchand[4], U. Marconi[15], C. Marin Benito[40], M. Marinangeli[43], P. Marino[43], J. Marks[12], G. Martellotti[26], M. Martin[6], M. Martinelli[43], D. Martinez Santos[41], F. Martinez Vidal[72], A. Massafferri[1], R. Matev[42], A. Mathad[50], Z. Mathe[42], C. Matteuzzi[20], A. Mauri[44], E. Maurice[7,b], B. Maurin[43], A. Mazurov[47], M. McCann[55,42], A. McNab[56], R. McNulty[13], J.V. Mead[54], B. Meadows[59], C. Meaux[6], F. Meier[10], N. Meinert[67], D. Melnychuk[31], M. Merk[27], A. Merli[21,42,q], E. Michielin[23], D.A. Milanes[66], E. Millard[50], M.-N. Minard[4], L. Minzoni[16,g], D.S. Mitzel[12], A. Mogini[8], J. Molina Rodriguez[1,x], T. Mombächer[10], I.A. Monroy[66], S. Monteil[5], M. Morandin[23], M.J. Morello[24,t], O. Morgunova[69], J. Moron[30], A.B. Morris[52], R. Mountain[61], F. Muheim[52], M. Mulder[27], D. Müller[56], J. Müller[10], K. Müller[44], V. Müller[10], P. Naik[48], T. Nakada[43], R. Nandakumar[51], A. Nandi[57], I. Nasteva[2], M. Needham[52], N. Neri[21,42,q], S. Neubert[12], N. Neufeld[42], M. Neuner[12], T.D. Nguyen[43], C. Nguyen-Mau[43,n], S. Nieswand[9], R. Niet[10], N. Nikitin[35], T. Nikodem[12], A. Nogay[69], A. Oblakowska-Mucha[30], V. Obraztsov[39], S. Ogilvy[53], D.P. O'Hanlon[50], R. Oldeman[22,f], C.J.G. Onderwater[68], A. Ossowska[29], J.M. Otalora Goicochea[2], P. Owen[44], A. Oyanguren[72], P.R. Pais[43], A. Palano[14], M. Palutan[18,42], A. Papanestis[51], M. Pappagallo[52], L.L. Pappalardo[16,g], W. Parker[60], C. Parkes[56], G. Passaleva[17,42], A. Pastore[14,d], M. Patel[55], C. Patrignani[15,e], A. Pearce[42], A. Pellegrino[27], G. Penso[26], M. Pepe Altarelli[42], S. Perazzini[42], D. Pereima[34], P. Perret[5], L. Pescatore[43], K. Petridis[48], A. Petrolini[19,h], A. Petrov[69], M. Petruzzo[21,q], E. Picatoste Olloqui[40], B. Pietrzyk[4], G. Pietrzyk[43], M. Pikies[29], D. Pinci[26], F. Pisani[42], A. Pistone[19,h], A. Piucci[12], V. Placinta[32], S. Playfer[52], M. Plo Casasus[41], F. Polci[8], M. Poli Lener[18], A. Poluektov[50], I. Polyakov[61], E. Polycarpo[2], G.J. Pomery[48], S. Ponce[42], A. Popov[39], D. Popov[11,42], S. Poslavskii[39], C. Potterat[2], E. Price[48], J. Prisciandaro[41], C. Prouve[48], V. Pugatch[46], A. Puig Navarro[44], H. Pullen[57], G. Punzi[24,p], W. Qian[50], J. Qin[63], R. Quagliani[8], B. Quintana[5], B. Rachwal[30], J.H. Rademacker[48], M. Rama[24], M. Ramos Pernas[41], M.S. Rangel[2], I. Raniuk[45,†], F. Ratnikov[37,aa], G. Raven[28], M. Ravonel Salzgeber[42], M. Reboud[4], F. Redi[43], S. Reichert[10], C. Remon Alepuz[72], V. Renaudin[7], S. Ricciardi[51], S. Richards[48], M. Rihl[42], K. Rinnert[54],

P. Robbe[7], A. Robert[8], A.B. Rodrigues[43], E. Rodrigues[59], J.A. Rodriguez Lopez[66],
A. Rogozhnikov[37], S. Roiser[42], A. Rollings[57], V. Romanovskiy[39], A. Romero Vidal[41,42],
M. Rotondo[18], M.S. Rudolph[61], T. Ruf[42], P. Ruiz Valls[72], J. Ruiz Vidal[72], J.J. Saborido Silva[41],
E. Sadykhov[34], N. Sagidova[33], B. Saitta[22,f], V. Salustino Guimaraes[62],
C. Sanchez Mayordomo[72], B. Sanmartin Sedes[41], R. Santacesaria[26], C. Santamarina Rios[41],
M. Santimaria[18], E. Santovetti[25,j], G. Sarpis[56], A. Sarti[18,k], C. Satriano[26,s], A. Satta[25],
D.M. Saunders[48], D. Savrina[34,35], S. Schael[9], M. Schellenberg[10], M. Schiller[53], H. Schindler[42],
M. Schmelling[11], T. Schmelzer[10], B. Schmidt[42], O. Schneider[43], A. Schopper[42], H.F. Schreiner[59],
M. Schubiger[43], M.H. Schune[7], R. Schwemmer[42], B. Sciascia[18], A. Sciubba[26,k],
A. Semennikov[34], E.S. Sepulveda[8], A. Sergi[47], N. Serra[44], J. Serrano[6], L. Sestini[23], P. Seyfert[42],
M. Shapkin[39], I. Shapoval[45], Y. Shcheglov[33], T. Shears[54], L. Shekhtman[38,w], V. Shevchenko[69],
B.G. Siddi[16], R. Silva Coutinho[44], L. Silva de Oliveira[2], G. Simi[23,o], S. Simone[14,d], M. Sirendi[49],
N. Skidmore[48], T. Skwarnicki[61], E. Smith[9], I.T. Smith[52], J. Smith[49], M. Smith[55],
l. Soares Lavra[1], M.D. Sokoloff[59], F.J.P. Soler[53], B. Souza De Paula[2], B. Spaan[10], P. Spradlin[53],
S. Sridharan[42], F. Stagni[42], M. Stahl[12], S. Stahl[42], P. Stefko[43], S. Stefkova[55], O. Steinkamp[44],
S. Stemmle[12], O. Stenyakin[39], M. Stepanova[33], H. Stevens[10], S. Stone[61], B. Storaci[44],
S. Stracka[24,p], M.E. Stramaglia[43], M. Straticiuc[32], U. Straumann[44], J. Sun[3], L. Sun[64],
K. Swientek[30], V. Syropoulos[28], T. Szumlak[30], M. Szymanski[63], Z. Tang[3], A. Tayduganov[6],
T. Tekampe[10], G. Tellarini[16,g], F. Teubert[42], E. Thomas[42], M.J. Tilley[55], V. Tisserand[5],
S. T'Jampens[4], M. Tobin[43], S. Tolk[49], L. Tomassetti[16,g], D. Tonelli[24],
R. Tourinho Jadallah Aoude[1], E. Tournefier[4], M. Traill[53], M.T. Tran[43], M. Tresch[44],
A. Trisovic[49], A. Tsaregorodtsev[6], P. Tsopelas[27], A. Tully[49], N. Tuning[27,42], A. Ukleja[31],
A. Usachov[7], A. Ustyuzhanin[37], U. Uwer[12], C. Vacca[22,f], A. Vagner[71], V. Vagnoni[15,42],
A. Valassi[42], S. Valat[42], G. Valenti[15], M. van Beuzekom[27], E. van Herwijnen[42], J. van Tilburg[27],
M. van Veghel[27], R. Vazquez Gomez[42], P. Vazquez Regueiro[41], C. Vázquez Sierra[27], S. Vecchi[16],
J.J. Velthuis[48], M. Veltri[17,r], G. Veneziano[57], A. Venkateswaran[61], T.A. Verlage[9], M. Vernet[5],
M. Vesterinen[57], J.V. Viana Barbosa[42], D. Vieira[63], M. Vieites Diaz[41], H. Viemann[67],
X. Vilasis-Cardona[40,m], M. Vitti[49], V. Volkov[35], A. Vollhardt[44], B. Voneki[42], A. Vorobyev[33],
V. Vorobyev[38,w], N. Voropaev[33], C. Voß[9], R. Waldi[67], J. Walsh[24], J. Wang[61], M. Wang[3],
Y. Wang[65], D.R. Ward[49], H.M. Wark[54], N.K. Watson[47], D. Websdale[55], A. Weiden[44],
C. Weisser[58], M. Whitehead[42], J. Wicht[50], G. Wilkinson[57], M. Wilkinson[61], M. Williams[58],
M.R.J. Williams[56], T. Williams[47], F.F. Wilson[51,42], J. Wimberley[60], M. Winn[7], J. Wishahi[10],
W. Wislicki[31], M. Witek[29], G. Wormser[7], S.A. Wotton[49], K. Wyllie[42], Y. Xie[65], M. Xu[65],
Q. Xu[63], Z. Xu[4], Z. Xu[3], Z. Yang[3], Z. Yang[60], Y. Yao[61], H. Yin[65], J. Yu[65,y], X. Yuan[61],
O. Yushchenko[39], K.A. Zarebski[47], M. Zavertyaev[11,c], L. Zhang[3], Y. Zhang[7], A. Zhelezov[12],
Y. Zheng[63], X. Zhu[3], V. Zhukov[9,35], J.B. Zonneveld[52], S. Zucchelli[15,e].

[1] *Centro Brasileiro de Pesquisas Físicas (CBPF), Rio de Janeiro, Brazil*
[2] *Universidade Federal do Rio de Janeiro (UFRJ), Rio de Janeiro, Brazil*
[3] *Center for High Energy Physics, Tsinghua University, Beijing, China*
[4] *Univ. Grenoble Alpes, Univ. Savoie Mont Blanc, CNRS, IN2P3-LAPP, Annecy, France*
[5] *Université Clermont Auvergne, CNRS/IN2P3, LPC, Clermont-Ferrand, France*
[6] *Aix Marseille Univ, CNRS/IN2P3, CPPM, Marseille, France*
[7] *LAL, Univ. Paris-Sud, CNRS/IN2P3, Université Paris-Saclay, Orsay, France*
[8] *LPNHE, Sorbonne Université, Paris Diderot Sorbonne Paris Cité, CNRS/IN2P3, Paris, France*
[9] *I. Physikalisches Institut, RWTH Aachen University, Aachen, Germany*
[10] *Fakultät Physik, Technische Universität Dortmund, Dortmund, Germany*
[11] *Max-Planck-Institut für Kernphysik (MPIK), Heidelberg, Germany*
[12] *Physikalisches Institut, Ruprecht-Karls-Universität Heidelberg, Heidelberg, Germany*
[13] *School of Physics, University College Dublin, Dublin, Ireland*
[14] *INFN Sezione di Bari, Bari, Italy*
[15] *INFN Sezione di Bologna, Bologna, Italy*

[16] INFN Sezione di Ferrara, Ferrara, Italy

[17] INFN Sezione di Firenze, Firenze, Italy

[18] INFN Laboratori Nazionali di Frascati, Frascati, Italy

[19] INFN Sezione di Genova, Genova, Italy

[20] INFN Sezione di Milano-Bicocca, Milano, Italy

[21] INFN Sezione di Milano, Milano, Italy

[22] INFN Sezione di Cagliari, Monserrato, Italy

[23] INFN Sezione di Padova, Padova, Italy

[24] INFN Sezione di Pisa, Pisa, Italy

[25] INFN Sezione di Roma Tor Vergata, Roma, Italy

[26] INFN Sezione di Roma La Sapienza, Roma, Italy

[27] Nikhef National Institute for Subatomic Physics, Amsterdam, Netherlands

[28] Nikhef National Institute for Subatomic Physics and VU University Amsterdam, Amsterdam, Netherlands

[29] Henryk Niewodniczanski Institute of Nuclear Physics Polish Academy of Sciences, Kraków, Poland

[30] AGH - University of Science and Technology, Faculty of Physics and Applied Computer Science, Kraków, Poland

[31] National Center for Nuclear Research (NCBJ), Warsaw, Poland

[32] Horia Hulubei National Institute of Physics and Nuclear Engineering, Bucharest-Magurele, Romania

[33] Petersburg Nuclear Physics Institute (PNPI), Gatchina, Russia

[34] Institute of Theoretical and Experimental Physics (ITEP), Moscow, Russia

[35] Institute of Nuclear Physics, Moscow State University (SINP MSU), Moscow, Russia

[36] Institute for Nuclear Research of the Russian Academy of Sciences (INR RAS), Moscow, Russia

[37] Yandex School of Data Analysis, Moscow, Russia

[38] Budker Institute of Nuclear Physics (SB RAS), Novosibirsk, Russia

[39] Institute for High Energy Physics (IHEP), Protvino, Russia

[40] ICCUB, Universitat de Barcelona, Barcelona, Spain

[41] Instituto Galego de Física de Altas Enerxías (IGFAE), Universidade de Santiago de Compostela, Santiago de Compostela, Spain

[42] European Organization for Nuclear Research (CERN), Geneva, Switzerland

[43] Institute of Physics, Ecole Polytechnique Fédérale de Lausanne (EPFL), Lausanne, Switzerland

[44] Physik-Institut, Universität Zürich, Zürich, Switzerland

[45] NSC Kharkiv Institute of Physics and Technology (NSC KIPT), Kharkiv, Ukraine

[46] Institute for Nuclear Research of the National Academy of Sciences (KINR), Kyiv, Ukraine

[47] University of Birmingham, Birmingham, United Kingdom

[48] H.H. Wills Physics Laboratory, University of Bristol, Bristol, United Kingdom

[49] Cavendish Laboratory, University of Cambridge, Cambridge, United Kingdom

[50] Department of Physics, University of Warwick, Coventry, United Kingdom

[51] STFC Rutherford Appleton Laboratory, Didcot, United Kingdom

[52] School of Physics and Astronomy, University of Edinburgh, Edinburgh, United Kingdom

[53] School of Physics and Astronomy, University of Glasgow, Glasgow, United Kingdom

[54] Oliver Lodge Laboratory, University of Liverpool, Liverpool, United Kingdom

[55] Imperial College London, London, United Kingdom

[56] School of Physics and Astronomy, University of Manchester, Manchester, United Kingdom

[57] Department of Physics, University of Oxford, Oxford, United Kingdom

[58] Massachusetts Institute of Technology, Cambridge, MA, United States

[59] University of Cincinnati, Cincinnati, OH, United States

[60] University of Maryland, College Park, MD, United States

[61] Syracuse University, Syracuse, NY, United States

[62] Pontifícia Universidade Católica do Rio de Janeiro (PUC-Rio), Rio de Janeiro, Brazil, associated to [2]

[63] University of Chinese Academy of Sciences, Beijing, China, associated to [3]

[64] School of Physics and Technology, Wuhan University, Wuhan, China, associated to [3]

[65] Institute of Particle Physics, Central China Normal University, Wuhan, Hubei, China, associated to [3]

[66] Departamento de Fisica , Universidad Nacional de Colombia, Bogota, Colombia, associated to [8]

[67] Institut für Physik, Universität Rostock, Rostock, Germany, associated to [12]

[68] Van Swinderen Institute, University of Groningen, Groningen, Netherlands, associated to [27]

[69]National Research Centre Kurchatov Institute, Moscow, Russia, associated to [34]

[70]National University of Science and Technology "MISIS", Moscow, Russia, associated to [34]

[71]National Research Tomsk Polytechnic University, Tomsk, Russia, associated to [34]

[72]Instituto de Fisica Corpuscular, Centro Mixto Universidad de Valencia - CSIC, Valencia, Spain, associated to [40]

[73]Los Alamos National Laboratory (LANL), Los Alamos, United States, associated to [61]

[a]Universidade Federal do Triângulo Mineiro (UFTM), Uberaba-MG, Brazil

[b]Laboratoire Leprince-Ringuet, Palaiseau, France

[c]P.N. Lebedev Physical Institute, Russian Academy of Science (LPI RAS), Moscow, Russia

[d]Università di Bari, Bari, Italy

[e]Università di Bologna, Bologna, Italy

[f]Università di Cagliari, Cagliari, Italy

[g]Università di Ferrara, Ferrara, Italy

[h]Università di Genova, Genova, Italy

[i]Università di Milano Bicocca, Milano, Italy

[j]Università di Roma Tor Vergata, Roma, Italy

[k]Università di Roma La Sapienza, Roma, Italy

[l]AGH - University of Science and Technology, Faculty of Computer Science, Electronics and Telecommunications, Kraków, Poland

[m]LIFAELS, La Salle, Universitat Ramon Llull, Barcelona, Spain

[n]Hanoi University of Science, Hanoi, Vietnam

[o]Università di Padova, Padova, Italy

[p]Università di Pisa, Pisa, Italy

[q]Università degli Studi di Milano, Milano, Italy

[r]Università di Urbino, Urbino, Italy

[s]Università della Basilicata, Potenza, Italy

[t]Scuola Normale Superiore, Pisa, Italy

[u]Università di Modena e Reggio Emilia, Modena, Italy

[v]MSU - Iligan Institute of Technology (MSU-IIT), Iligan, Philippines

[w]Novosibirsk State University, Novosibirsk, Russia

[x]Escuela Agrícola Panamericana, San Antonio de Oriente, Honduras

[y]Physics and Micro Electronic College, Hunan University, Changsha City, China

[z]Lanzhou University, Lanzhou, China

[aa]National Research University Higher School of Economics, Moscow, Russia

[†]Deceased